




An AHP GIS-based Methodology for the Stability Assessment of the Djebel El Ouahch Collapsees on the Numidian Flysh Formation in Northeast Algeria's Constantine Region

Nadjet Bouragba^{1,2,3} , Riheb Hadji^{2,3*} , Abdelmadjid Chouabbi^{1,4} 

¹ Department of Geology, Faculty of Earth Sciences, Badji Mokhtar-Annaba University, Annaba, Algeria.

² Laboratory of Applied Research in Engineering Geology, Geotechnics, Water Sciences, Environment, UFAS, Algeria

³ Department of Earth Sciences, Institute of Architecture and Earth Sciences, University of Farhat Abbas, Setif, Algeria

⁴ Laboratory of Geodynamics and Natural Resources, Badji Mokhtar-Annaba University, Annaba, Algeria

bngeologie@gmail.com (N.B.); hadjirihab@gmail.com (R.H.); mchouabbi@yahoo.fr (A.C.)

Received: 30 September 2023; Revised: 1 December 2023; Accepted: 16 December 2023;

Published online: 20 December 2023

ABSTRACT: This study presents a comprehensive investigation into the factors underlying the collapse incident that occurred in the Jebel El Ouahch Tunnel in the Numidian flysch, Constantine region, Northeast Algeria. This methodology focuses on evaluating landslide susceptibility through the application of the Analytic Hierarchy Process (AHP) along the reconfigured path of the collapsed A1 highway tunnel section in the Constantine region of northeastern Algeria. Various influential factors contributing to landslides were analyzed, including lithofacies, slope gradient, slope aspect, elevations, fault density, plan curvature, distance from streams, and distance from roads. Utilizing a Geographic Information System (GIS), these eight causative factors were prepared for assessment. The findings indicate that slope gradient and lithology play pivotal roles as primary controlling factors in landslide susceptibility. The model exhibited a commendable success rate of 93% in predicting landslide susceptibility, as demonstrated by the area under the curve (AUC) plot generated from the landslides susceptibility map. Most of the new road falls within the highly susceptible area to landslides. This validated model can serve as an effective tool for mapping landslide susceptibility zones along the newly established road path following the collapsed tunnel. Moreover, its applicability extends to similar environments, showcasing its potential as a valuable resource for hazard assessment and planning in comparable terrains. The deviation road, as well as tunnel T01 of the A1 highway, is in a state of proven instability. It is certain that they will experience continuous, recurrent, and intense landslides. A radical solution to all the geotechnical issues plaguing this section of the highway is to reroute it far away from the Subnumidian formations. A deeper comprehension of the geological and geotechnical intricacies in challenging terrains can significantly enhance the safety and reliability of transportation networks in these demanding contexts.

KEYWORDS: tunnel collapse, geological complexities, landslide susceptibility, Analytic Hierarchy Process, construction hazards.

TO CITE THIS ARTICLE: Bouragba, N., Hadji, R., & Chouabbi, A. (2023). An AHP GIS-based Methodology for the Stability Assessment of the Djebel El Ouahch Collapsees on the Numidian Flysh Formation in Northeast Algeria's Constantine Region. *Central European Journal of Geography and Sustainable Development*, 5(2), 24–45. <https://doi.org/10.47246/CEJGSD.2023.5.2.2>

1. INTRODUCTION

Highway tunnels are vital for facilitating transportation and sustainable development in the mountainous terrains of Mediterranean countries. However, these regions pose significant challenges due to their complex geological, geotechnical, and hydrological conditions.

The morpho-structural context contributes to the frequent occurrence of collapse disasters in tunnel construction, resulting in substantial economic losses (Zhang et al., 2015; Zahri et al., 2016; Qiao et al., 2020). The intricate geological composition and dynamic hydrological systems in these areas make tunnel construction particularly vulnerable to collapse incidents. These disasters not only disrupt the construction process but also impose substantial financial burdens due to the extensive damages incurred.

* Corresponding author: hadjirihab@gmail.com; Tel.: +213 561 474 453

Therefore, addressing these challenges demands a comprehensive understanding of the geological complexities to develop robust engineering solutions. Enhancing the resilience of tunnel infrastructures through advanced construction techniques, innovative monitoring systems, and meticulous risk assessment strategies is imperative (Chen et al., 2022). By integrating scientific knowledge and technological advancements, it becomes possible to mitigate the risks associated with tunnel collapses, ultimately ensuring safer and more sustainable tunnel infrastructure in these challenging landscapes. There are many factors that can cause construction collapse in underground tunneling. Among them, some may stem from internal and external influences. Internal factors encompass design flaws, planning errors, and construction defects, including inadequacies in the temporary tunnel lining. Conversely, external factors relate to inadequate control over ground characteristics, including earthquakes, high-stress conditions, and water inflow (Kerbati et al., 2020; Boubazine et al., 2022; Benyoucef et al., 2023).

Several research studies have extensively investigated these deformations, shedding light on their underlying mechanisms and causes (Leichnetz, 1990; Hoek, 2001; Bonini & Barla, 2012; Feng & Jimenez, 2015; Lin et al., 2017; Kallel et al., 2018; Bagwan et al., 2023). An extensive review of the academic literature on landslide prediction and management highlights a wide range of techniques used for assessing susceptibility to geological hazards, particularly landslides (Guzzetti, 2021). These methodologies encompass quantitative, semi-quantitative, and qualitative approaches, providing both direct and indirect means of estimating and zoning landslide susceptibility. Quantitative methods include heuristic direct estimation, as well as deterministic, statistical, and probabilistic models. Researchers and practitioners have access to a multitude of bivariate and multivariate techniques, such as Frequency ratio (FR), Linear indexing (LI), Weighted evidence (WoE), Artificial neural network (ANN), Logistic regression (LR), and Analytic hierarchy process (AHP), among others (Conforti & Ietto, 2021). The diverse range of methodological options highlights the effectiveness of utilizing GIS techniques to evaluate and classify landslide hazards (Goetz et al., 2015; Juliev et al., 2019). Moreover, the integration of artificial intelligence (AI) and data mining (DM) techniques holds great promise for enhancing the field of landslide susceptibility assessment, offering unprecedented levels of relevance and validity (Zêzere et al., 2017; El Mekki et al., 2017; Reichenbach et al., 2018; Mahdadi et al., 2018; Achour et al., 2021; Manchar et al., 2022; Taib et al., 2022, 2023a, b).

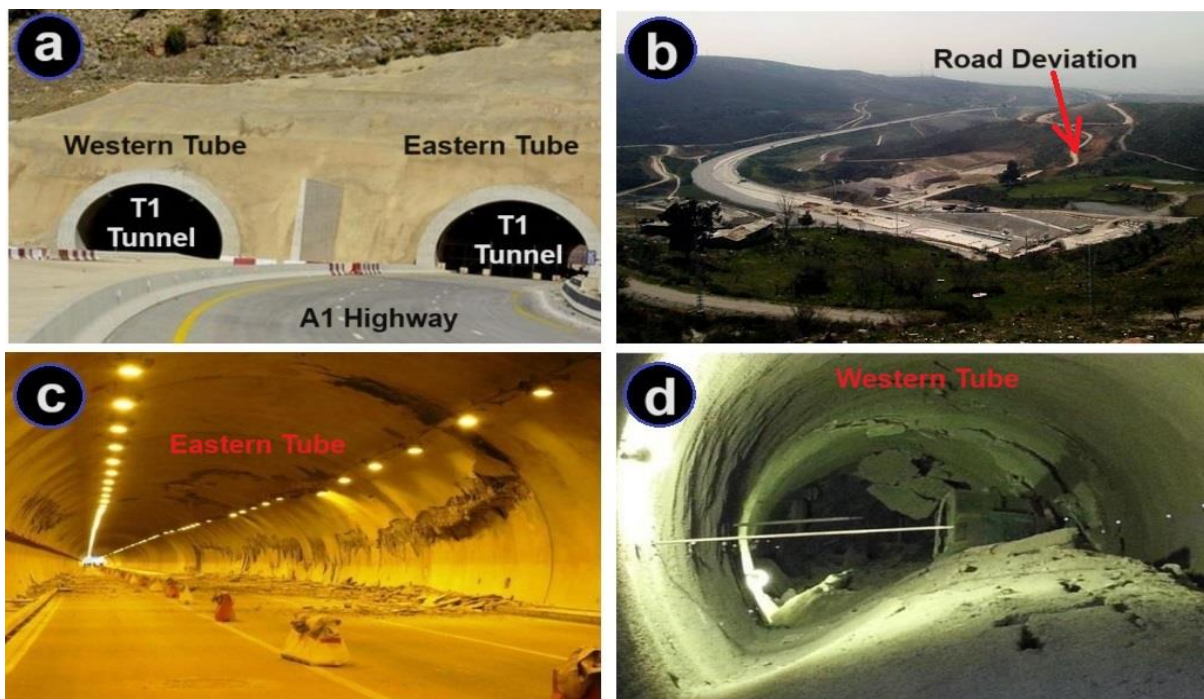


Figure 1. (a) Western Entrance of Tunnel T1. (b) Mountain bypass of the A1 highway route. (c) Partial collapse of the Right Tube (East). (d) Total collapse of the Left Tube (West).

Source: Berkane et al. (2022), COSIDER SPA, Highway Management Agency (AGA).

In mountainous regions of the Algerian Atlas chain, tunnels play a crucial role in ensuring mobility and fostering socio-economic development. The Jebel El Ouahch Tunnel, situated in Algeria's eastern Tell region within the Numidian Chain, traverses unstable lithological formation comprising argillite in the basement, sandstone-clay intercalations in the middle, and grey marl at the top (Figure 1a) (Karim et al., 2019). This region is particularly prone to gravitational disturbances due to chaotic formations within the Numidian Nappe (Kimour et al., 2023). On January 1, 2014, during excavation operations, a sudden collapse occurred in the left tube (West) of tunnel T1, part of the A1 highway between PK 206+152 and PK 206+265, spanning a distance of 113m (Figure 1a, c, d). This collapse not only damaged the two tubes but also led to severe cracks in the final lining along PK 206+199 to 262, covering a distance of 63m (Kitchah et al., 2021). This alarming incident prompted extensive geoenvironmental works to investigate the root causes and origins of the observed local disorders while traversing the sub-Numidian clays (Dahoua et al., 2017a; Fredj et al., 2020; Saadoune et al., 2020). To link both ends of the collapsed tunnel section and ensure the durability of traffic flow, a hasty solution was initiated by the construction of a 12.41 km temporary sinuous deviation over a steep relief between PK 205+393.000 and PK 207+284.500.

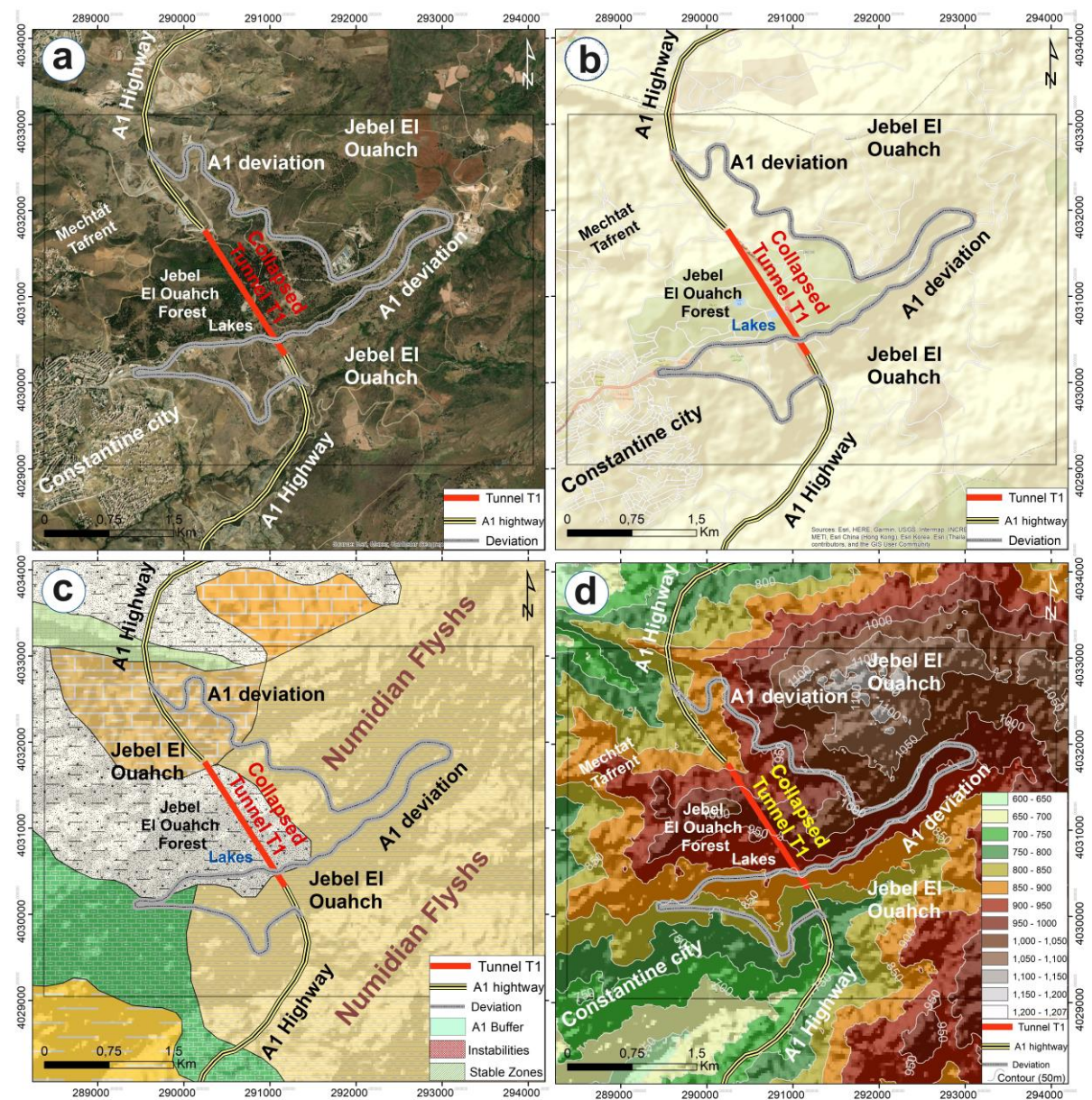


Figure 2. (a) The new Djebel El-Ouahch deviation on satellite images. (b) The new Djebel El-Ouahch deviation on street map. (c) The new Djebel El-Ouahch deviation on numidian (beige) formations. (d) The new Djebel El-Ouahch deviation on steep landscape (DEM).

However, due to landslides occurring along the new route, reinforcement work was necessary, involving the installation of over 1,000 piles across the 12.41 km stretch (Fig. 1b). The Djebel El-Ouahch deviation (Figure 2) required a public investment of more than 10 million USD, entrusted to national companies following the withdrawal of the Japanese consortium. The primary objective of this study was to identify viable solutions to prevent similar incidents in the future, including assessing the susceptibility of the new route to landslides and prioritizing risk into different classes, particularly those requiring immediate intervention. Despite technical and technological efforts, the issue remains unresolved, necessitating further scientific investigation (Manchar et al., 2018; Anis et al., 2019). Semi-quantitative methods utilizing Geographic Information Systems (GIS) have become integral in assessing geological hazards. The Analytic Hierarchy Process (AHP), pioneered by Saaty in 1977, remains an indispensable tool for mapping landslides due to its enduring relevance and efficacy. Its versatility is evident in various applications, including site selection, suitability analysis, regional planning, and the assessment of landslide susceptibility (Ayalew et al., 2005). Numerous researchers have successfully employed AHP for landslide susceptibility mapping, demonstrating its robustness and applicability (Achour et al., 2017). AHP involves constructing a hierarchical structure of decision elements or factors, followed by systematic comparisons among these elements. This method facilitates a structured and rigorous approach to decision-making, enabling a comprehensive evaluation of landslide susceptibility and contributing factors within a geographic context. This study provides valuable insights into the intricate geological complexities contributing to the tunnel collapse event, laying the groundwork for effective strategies to mitigate such hazards in future tunnel constructions. The findings of this research hold significant potential to improve the safety and sustainability of tunnel infrastructure projects in regions facing similar geological challenges.

2. STUDY AREA

The study area is located in Constantine city, a major metropolis in northeastern Algeria, approximately 350 km away from the capital, Algiers (Figure 3).



Figure 3. Geographical location of the study area in Algeria map.

The region is traversed by the A1 (E-W highway), situated on the eastern side of the chief town. This highway passes through a mountainous terrain covered with dense forests, known as Jebel El Ouahch Park. To overcome the steep relief between PK 205+393.000 and PK 207+284.500, the engineers opted to construct a two-tube tunnel spanning a distance of 1,891.5 m (Figure 4a).

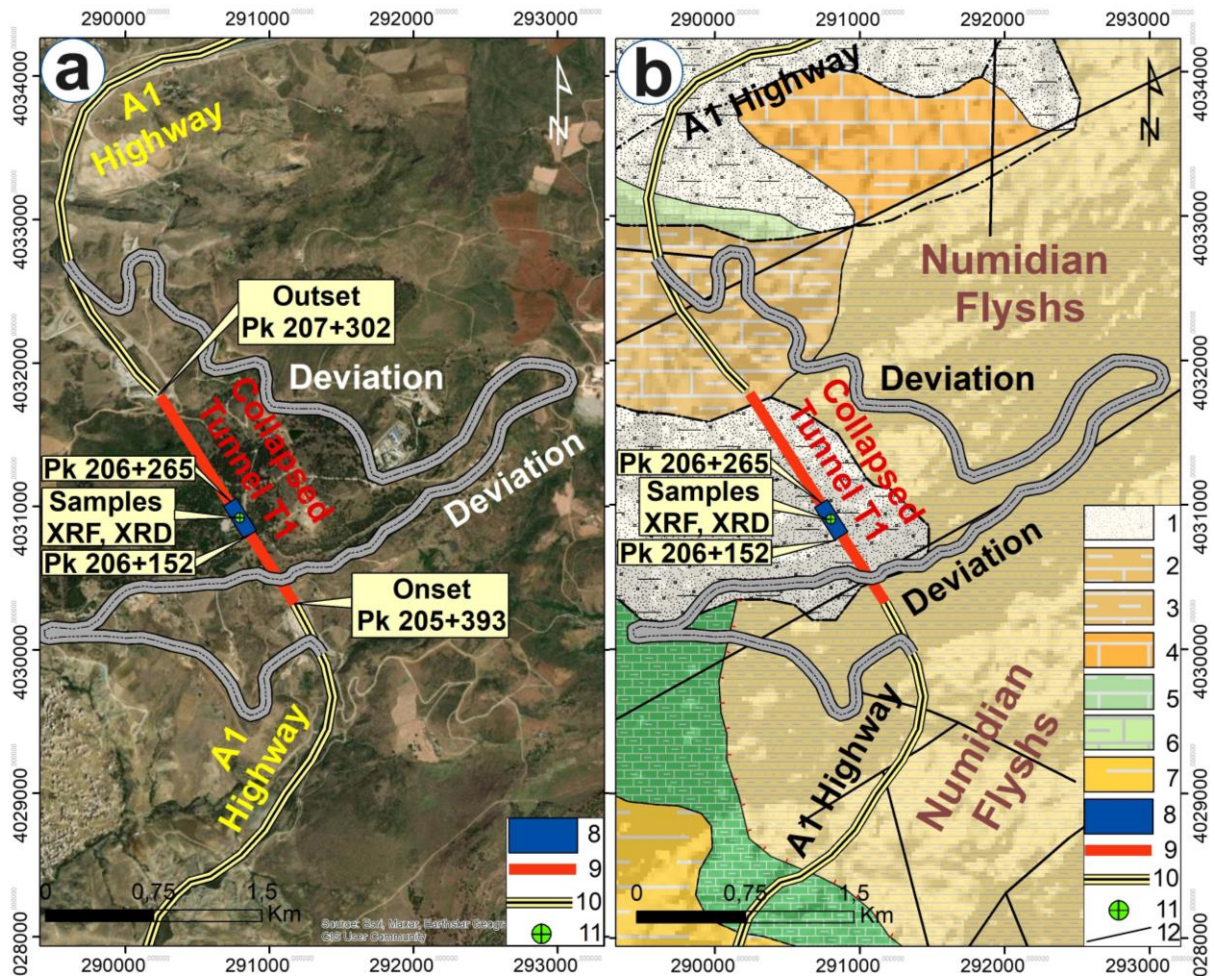


Figure 4. (a) Satellite image of the study area, showing the tunnel (T1), the highway (A1) and the deviation. (b) Simplified geological map of the study area, with samples points. [Legend: 1 = Quaternary (Holocene): Current alluvial deposits, occasional slope debris, and piedmont accumulations. 2 = Oligocene: Series of clays at the base and sandstones at the top. 3 = Paleocene-Maastrichtian: Marls and marl-limestones. 4 = Lower and Middle Eocene (Ypresian and Lower Lutetian): Limestones with flint and marl-limestones, sometimes with gypsum. 5 = Lower Cretaceous (Aptian): Marls, shales, and limestones. 6 = Upper Cretaceous (Coniacian-Maastrichtian): Grey marls and limestone beds at the top. 7 = Middle Eocene (Upper Lutetian): Marls, clays, and locally conglomerates. 8 = Collapsed zone. 9 = Tunnel T1. 10 = A1 Highway. 11 = XRD and XRF samples. 12 = Faults.]

The Eastern (right) tube of the tunnel was completed and opened to traffic in April 2013, while the West tube (left tube) was still under excavation. However, an unfortunate incident occurred on January 1, 2014, when the West tube suffered a catastrophic collapse during construction, causing significant disruptions and damage to the operational East tube, which had been in service for only a few months. As a result of this disaster, the East tube had to be closed off to ensure traffic safety. To address the closure of the East tube, a temporary sinuous road was hastily constructed as an alternate route. This detour, extending over 12.41 km, winds its way up the slopes of Jebel El Ouahch, starting from the southern entrance and exiting on the northern side of the tunnel. However, this temporary road poses a considerable risk, particularly for heavy vehicles, and requires immediate attention. The northeastern region of Constantine showcases a fascinating and intricate geological landscape, characterized by brittle tectonics. This complexity is attributed to the presence of various thrust sheets, including the Numidian,

Tellian, and Constantinois neritic sheets. The area is of significant importance as it houses a major highway, with Tunnel T1 serving as a notable engineering feat. Jebel El Ouahch, a prominent mountain in the region, is primarily composed of massive Numidian sandstones, which are visually impressive and structurally significant. As we venture towards the southern part of this mountainous massif, an intriguing geological phenomenon unfolds - the presence of Massylian flysch formations (Zerzour et al., 2020, 2021; Benmarce et al., 2021). These flysch deposits, characterized by sedimentary rocks containing microbreccias, provide valuable clues about the ancient environmental conditions and depositional processes. Moreover, these flysch layers rest upon extensively deformed Ultra-Tellian formations, a geological unit that spans a considerable timespan from the Barrémian to the Lower Lutetian periods. The dating of these formations has been established through the work of Moretti et al. (1991). Notably, underneath the towering Numidian sandstone of Jebel El Ouahch, we find the exposure of sub-Numidian Tubotomaculum claystone on the eastern side of the site. These claystones offer insights into the geological history and can reveal crucial information about the rock's origin, composition, and formation processes (Hadji et al., 2013; Boulemia et al., 2021), (Figure 4b). Samples were taken from the core drillings carried out at depths ranging from 107m to 128m. An examination of the lithological sections of the drill revealed nearly identical lithology for all three samples. The top formation (from 0 to 18m) consists of sandy and loamy clays, sandy loam, and clayey sands, followed by monotonous lithology down to 128m, composed of clays. These clays exhibit a grayish, sometimes greenish hue, with a schistose appearance. The schistosity planes are shiny and smooth, marked by the presence of fine white material. Occasionally, these clays display reddish and greenish patina. This description was supplemented by observations made inside the West tube (collapsed tunnel) and in the field. At this clayey level, we conducted sampling by collecting three samples at different depths for each drilling. Samples of sandstone were also collected from the sandstone layers to prepare thin sections for the study of their mineral composition. Observation of the thin sections under a polarizing microscope revealed that these sandstones are primarily composed of 95% quartz grains. These grains are sub-rounded and have a microscopic size. There is also a presence of biotite, but in very low percentages, sometimes found within the quartz grains.

3. RESEARCH METHODS

3.1. Landslides susceptibility mapping

The study began with the preparation of a landslide inventory map based on field surveys. Analytic hierarchy process was used for landslide susceptibility mapping for the studied area in a GIS environment. The statistical analysis is carried out utilizing SPSS package. After reclassification using the natural break classification method, the resulted maps represent the final landslide susceptibility models. Finally, validation of the model was carried out to select the valid land slide susceptibility map for the study area. The followed methodology of the work is shown in Figure 5.

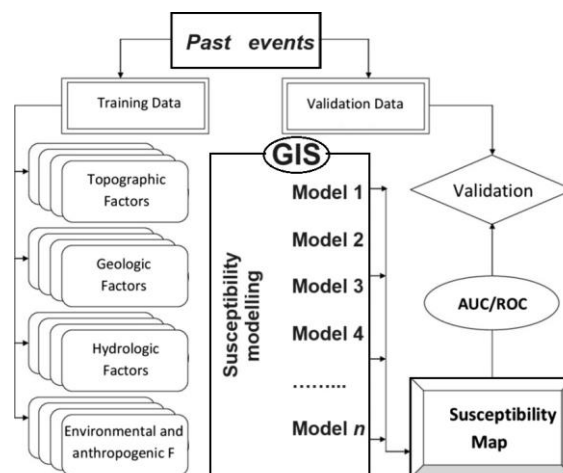


Figure 5. The methodological flow chart used in the GIS modelling.

3.1.1. Analytic hierarchy process

The Analytic Hierarchy Process (AHP) serves as a multi-criteria decision-making method that involves pairwise comparisons between various factors represented in a matrix to assign weights to each factor and establish a consistency ratio (Saaty, 1980). This process determines the relative importance of each factor to all other factors. In the AHP methodology, each factor is assessed against every other factor by assigning values typically ranging from 1 to 9 for factors with a direct relationship. Conversely, reciprocal values between $1/2$ and $1/9$ are used when the relationship between factors is inversely proportional. The essential steps in the AHP procedure include standardizing the factors, determining the weight of each factor, and aggregating the criteria. Initially, standardization ensures that factors and their spatial representations are aligned on a common scale, facilitating meaningful comparisons. Subsequently, a comparison matrix is constructed, enabling the assessment of each factor's importance to others. The quality of these comparisons is evaluated using the consistency ratio, which is calculated based on the consistency index and the random index. An acceptable level of consistency is indicated by a consistency ratio of less than 10%. A lower consistency ratio implies that the computed weights for each factor are reliable. Utilizing a weighted linear combination, the landslide susceptibility map is generated. This involves overlaying layers representing controlling factors and multiplying them by their corresponding weight values, providing a comprehensive depiction of areas prone to landslides based on the amalgamation of these influential factors.

3.1.2. Conditioning factors

The selection of factors for landslide susceptibility mapping lacks rigid guidelines but revolves around key parameters such as lithofacies and slope angle, which have been proven to be highly influential in the genesis and triggering of instabilities. This method has been applied by various researchers (Hadji et al., 2014a, b, 2016, 2017; Dahoua et al., 2018).

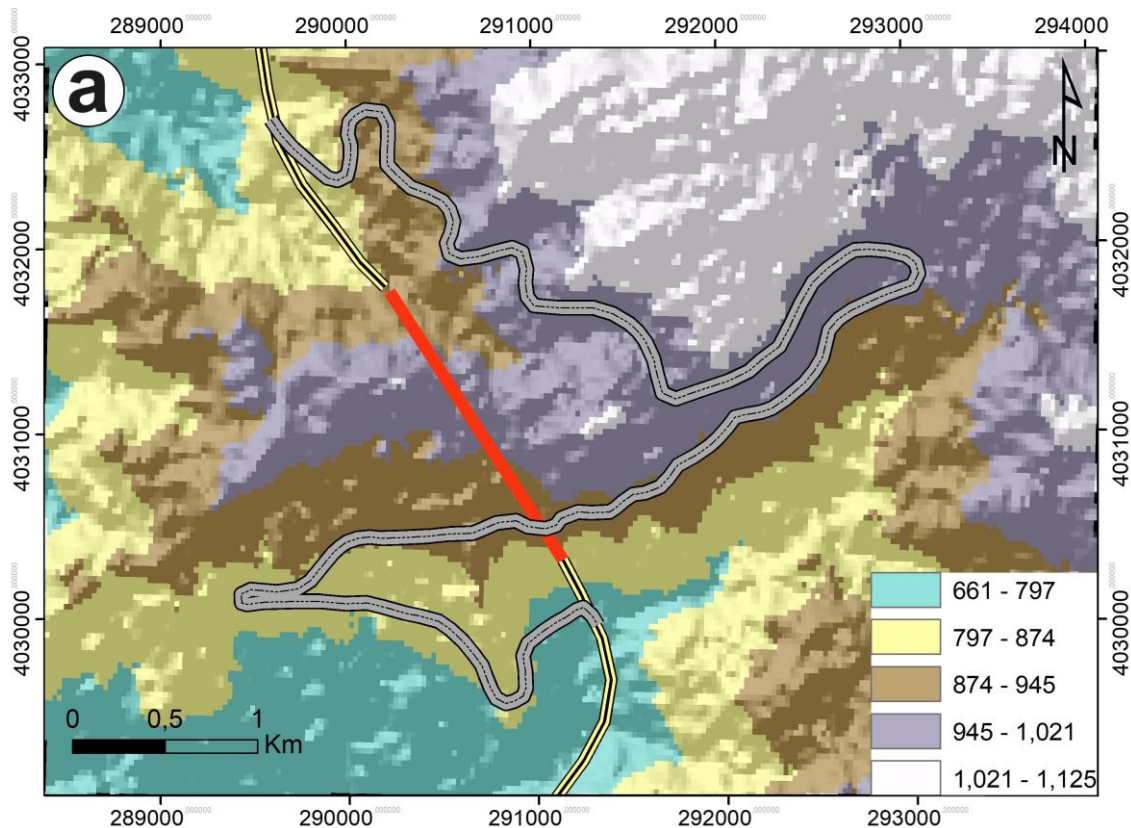


Figure 6. (a) Elevation map.

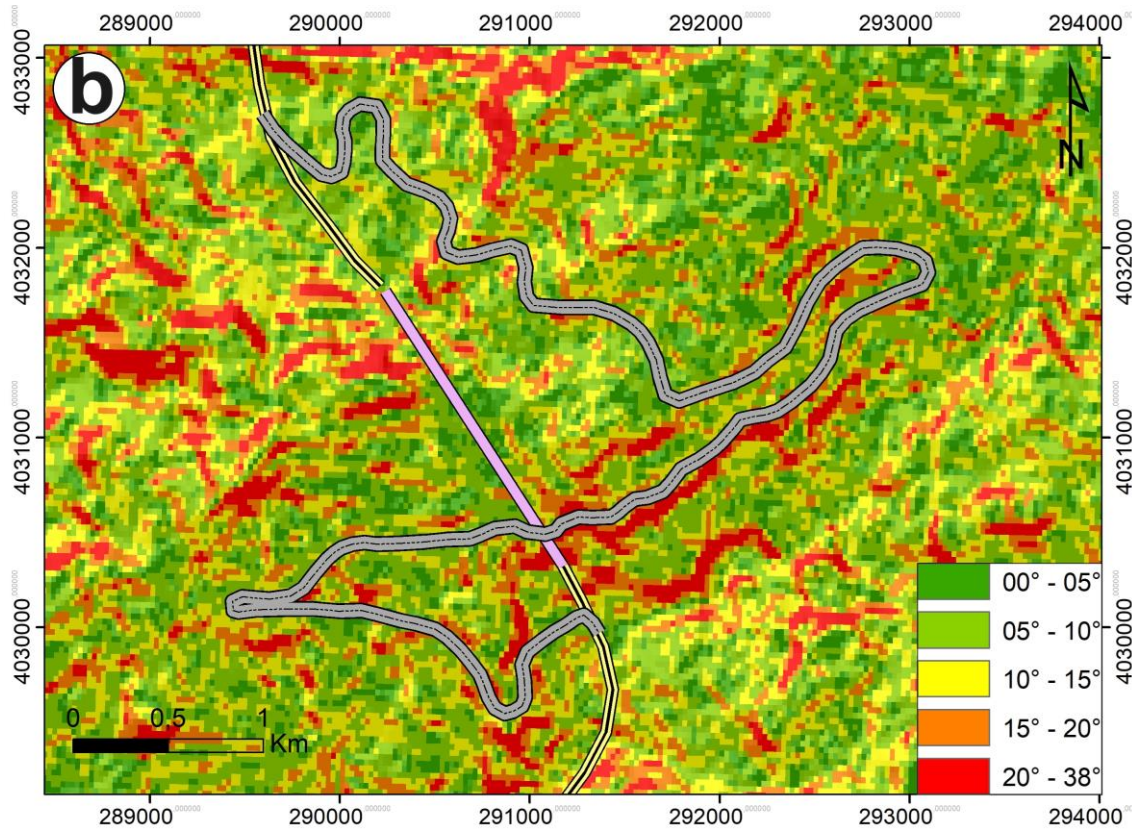


Figure 6. (b) Slope map.

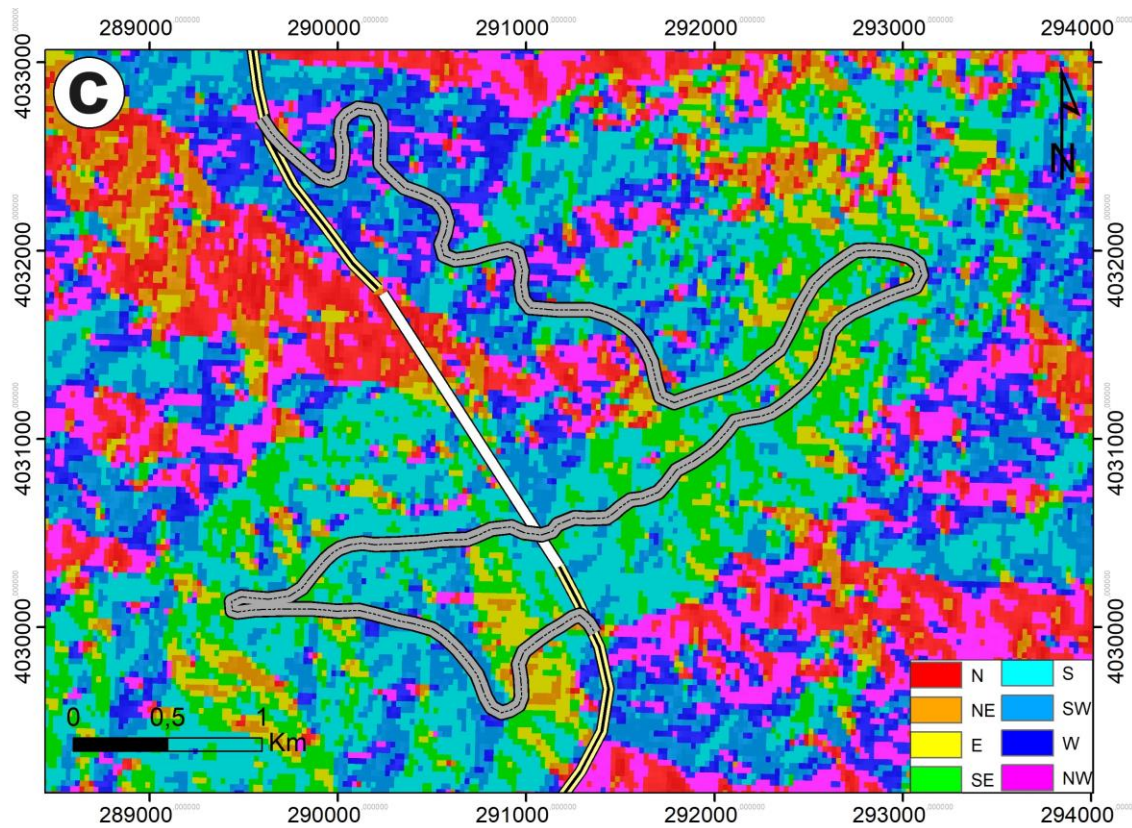


Figure 6. (c) Aspect map.

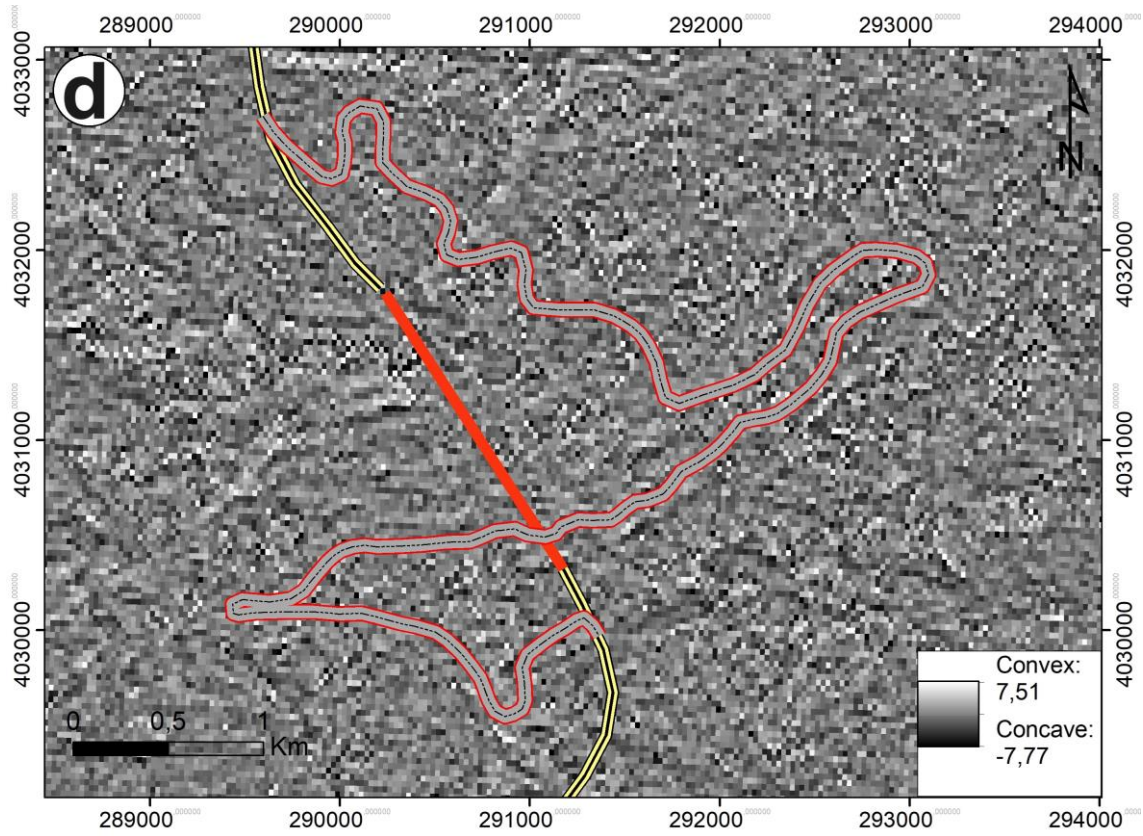


Figure 6. (d) Plan curvature map.

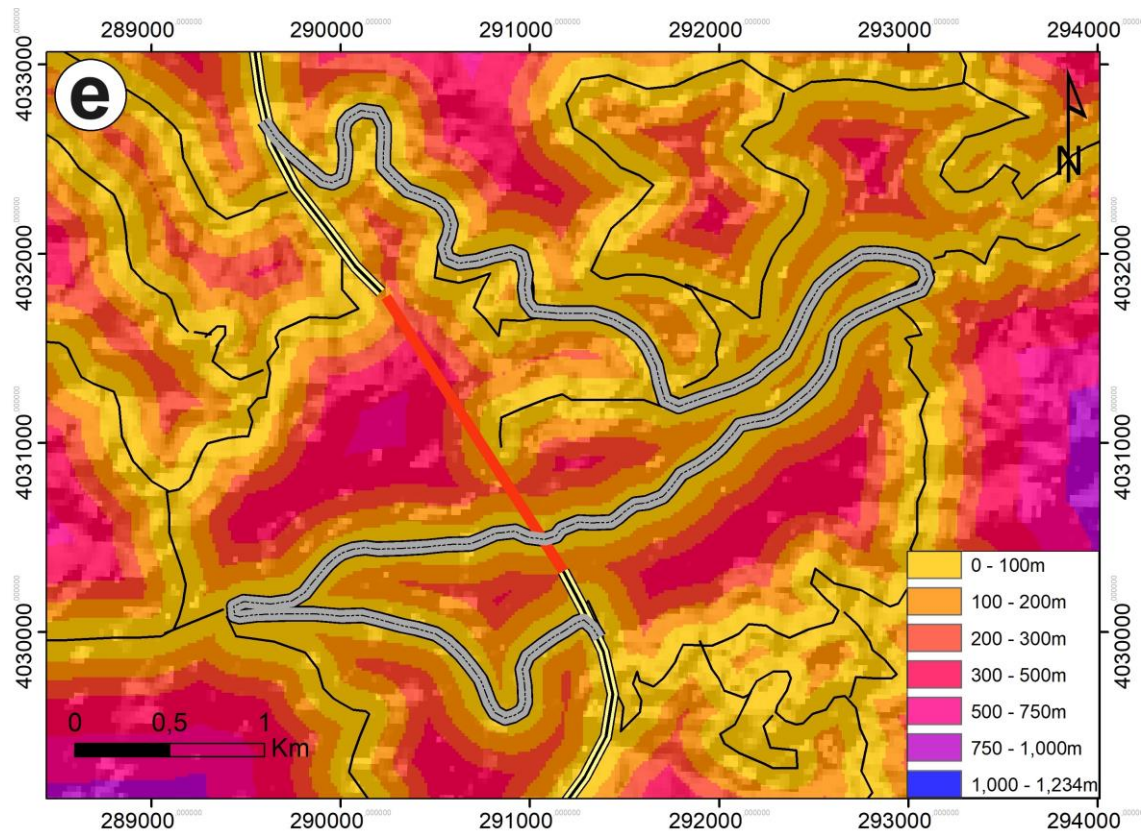


Figure 6. (e) Distance to roads map.

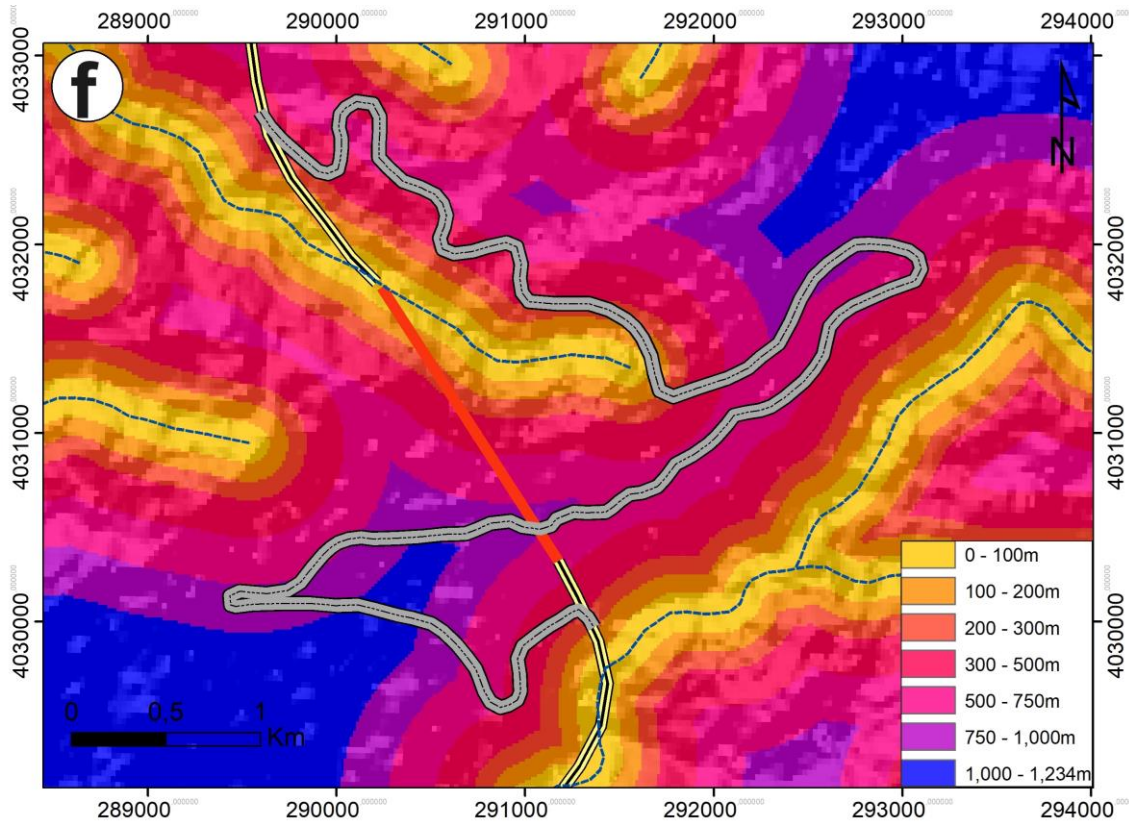


Figure 6. (f) Distance to streams map.

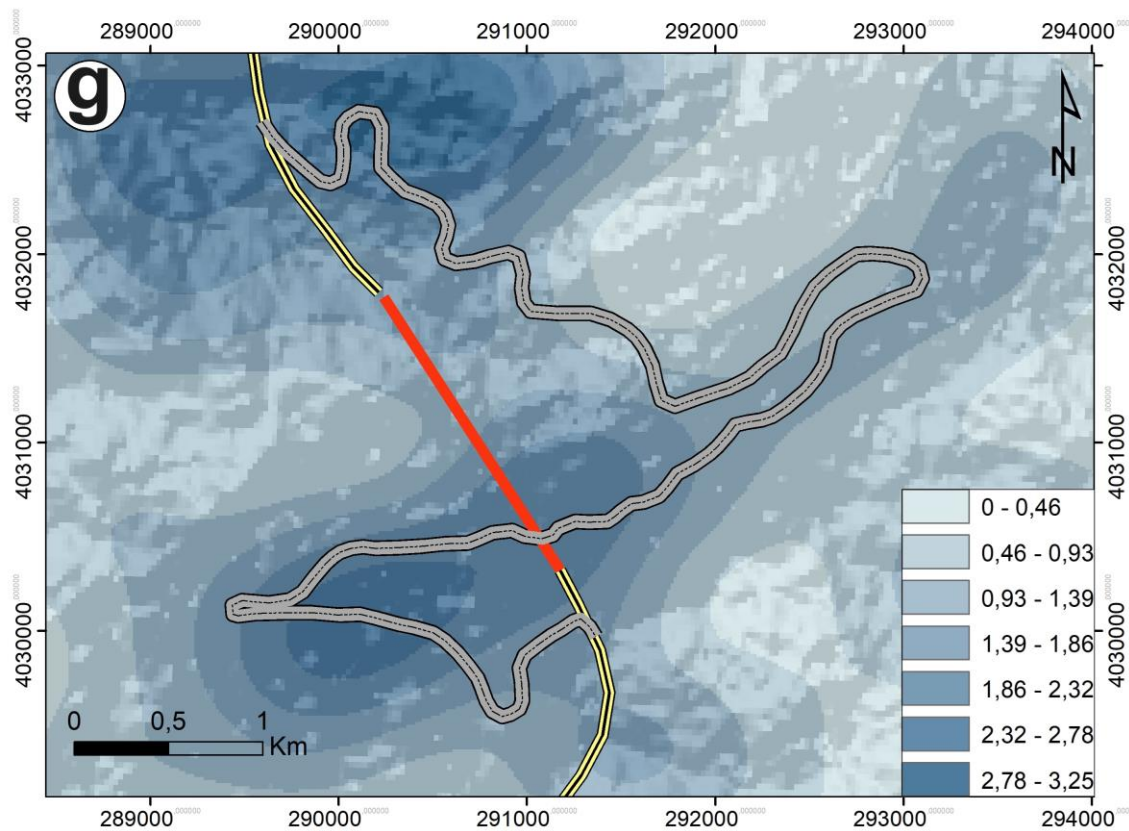


Figure 6. (g) Fault density map.

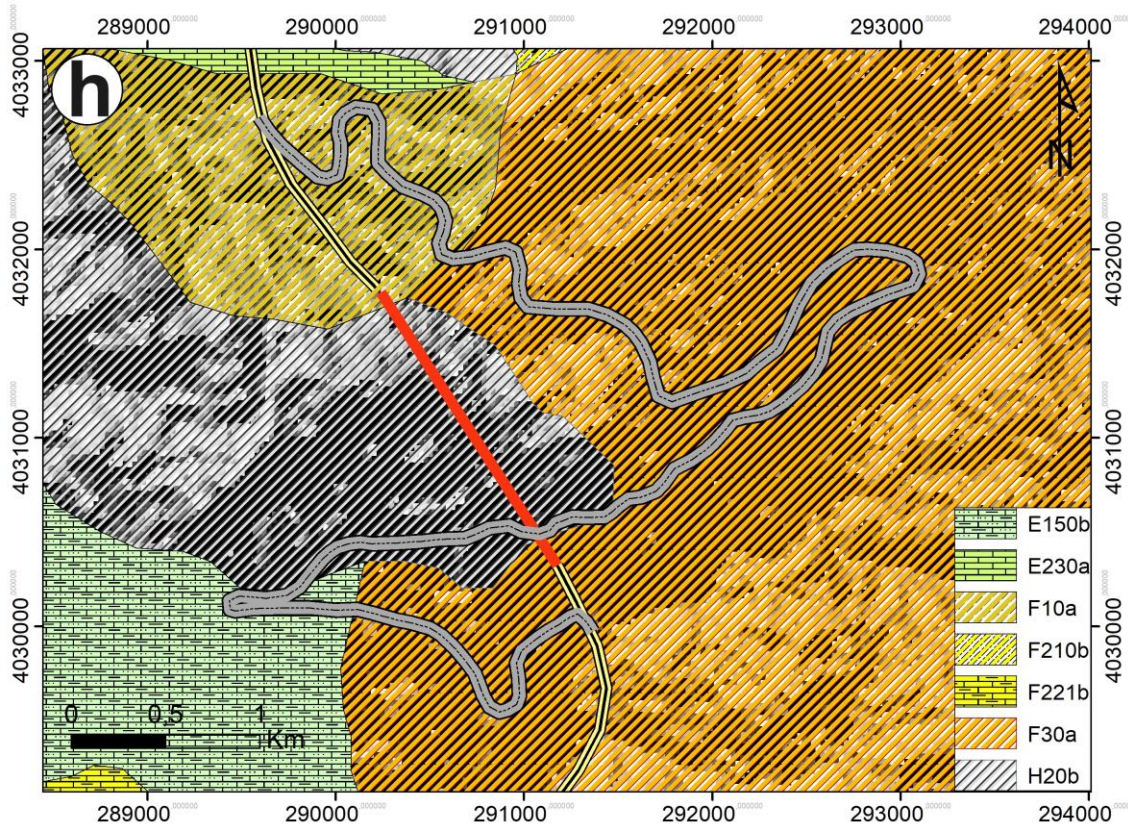


Figure 6. (h) Lithofacies map.

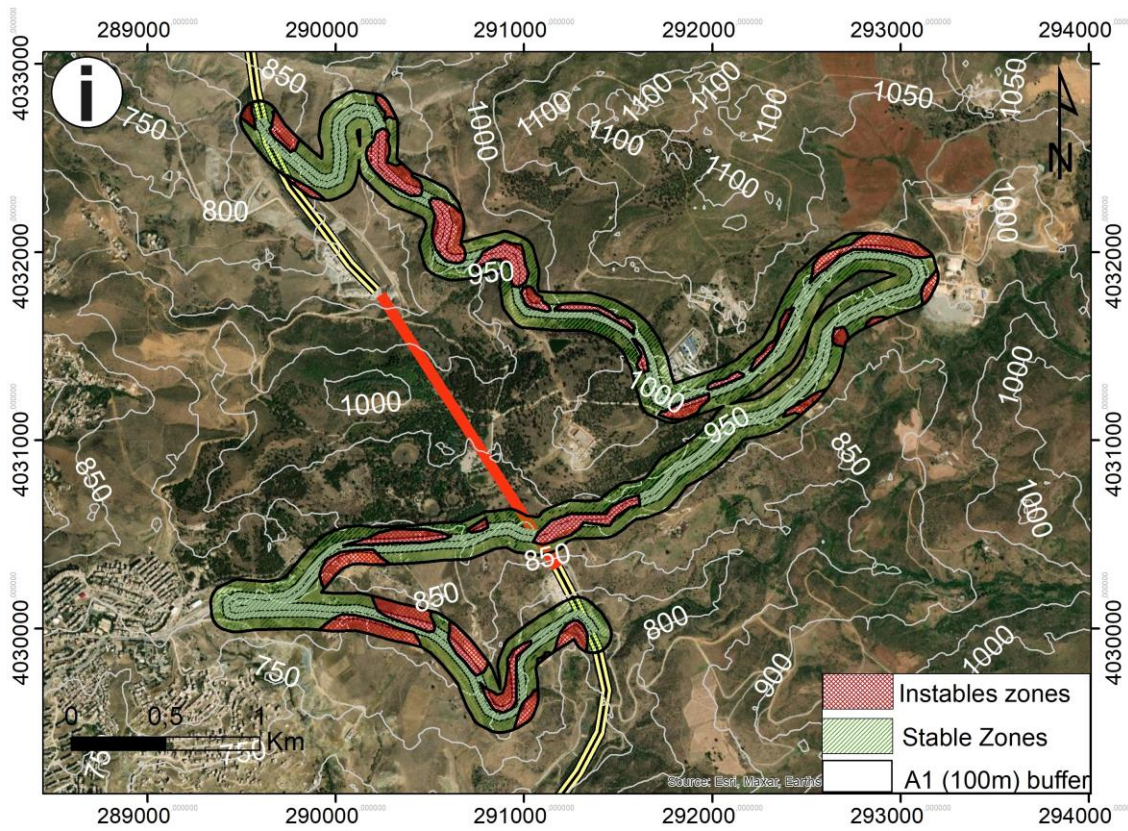


Figure 6. (i) Landslides inventory map.

Factors chosen for landslide susceptibility assessment must meet specific criteria; they need to be operational, comprehensive, and non-redundant attributes. Based on these criteria, eight pivotal

predisposing factors were considered in this study, encompassing lithofacies, slope gradient, slope aspect, elevations, fault density, plan curvature, distance from streams, and distance from roads (Zeqiri et al., 2019; Ncibi et al., 2021; Hamed et al., 2023). These factors are compared to the landslides inventory map (Fig. 6i).

Lithofacies significantly influence landslide predisposition and triggering due to variations in the strength and permeability of rocks and soils. In this study, lithostratigraphic outcrops were extracted from the 1:50,000 geological map of Constantine. These lithostratigraphic outcrops comprise various formations including Quaternary (Holocene) deposits, Oligocene clay series with sandstones, Paleocene-Maastrichtian marls and marl-limestones, Lower and Middle Eocene limestone variations, Lower Cretaceous marls, shales, and limestones, Upper Cretaceous grey marls and limestone beds, and Middle Eocene marls, clays, and conglomerates (Figure 6h).

Morphological factors such as slope gradient, slope aspect, and terrain elevation play pivotal roles in landslide control (Figure 6a, b, c). These parameters were derived from the digital elevation model and categorized into ascending classes using the Jenks method and field observations (Achour et al., 2020).

Fault lineaments were digitized from the geological map of Constantine and fieldwork. Increased fault density heightens the likelihood of landslides (Figure 6g). Additionally, the construction of roads involving cutting and filling the embankments can trigger slope instabilities. The distance from roads was factored into the assessment through a multiple-buffer procedure (Figure 6e).

Streams can adversely affect slope stability through erosion or saturation of the toe materials, reducing their shear resistance. For this study, a distance from streams map was categorized into five classes: 0–50 m, 50–100 m, 100–250 m, 250–500 m, and >500 m (Figure 6f). Furthermore, the concavity and convexity of slopes also play a crucial role in water flow and infiltration conditions (Figure 6d).

3.2. Geologic characters

3.2.1. X-ray diffraction (XRD) analysis

The fundamental design of an X-ray diffractometer (XRD) consists of a monochromatic radiation source and an X-ray detector positioned on a graduated circle at the center of a powder specimen. There are divergent slits placed between the X-ray source and the specimen, as well as between the specimen and the detector. These slits serve multiple purposes, including limiting scattered radiation (non-diffracted), reducing background noise, and collimating the radiation. To ensure synchronized movement, the detector and specimen holder are mechanically connected to a goniometer. This setup enables the detector to rotate through 2θ degrees while the specimen rotates through θ degrees, maintaining a fixed 2:1 ratio (Figure 7).

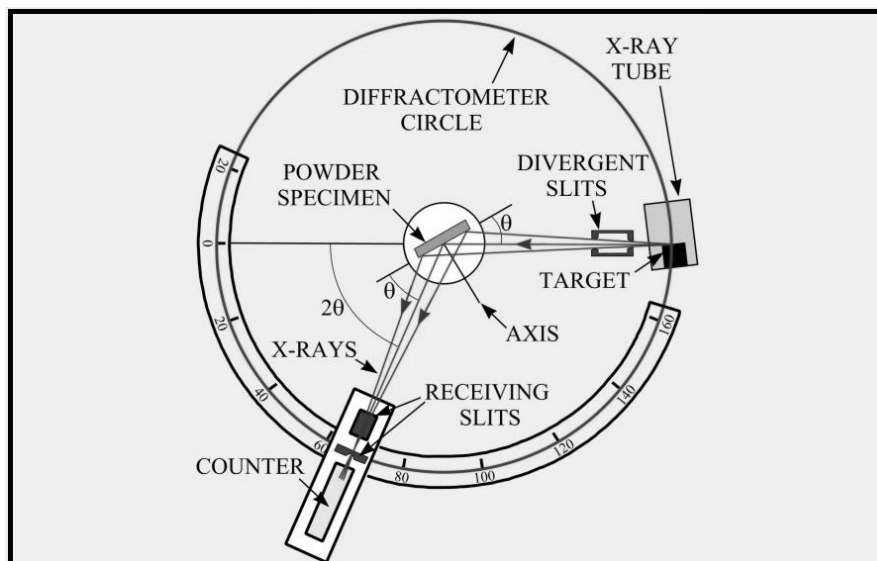


Figure 7. The USGS XRD protocol Schemes (Cullity, 1956).

Based on the U.S. Geological Survey Open-File Report 01-041, our investigation began with XRD analysis of powdered samples. These samples were obtained through mechanical grinding and meticulously analyzed to discern the crystalline phases present in each specimen. Moreover, oriented thin sections were meticulously prepared to enhance the identification of clay minerals within a fraction smaller than 80 μm . These thin sections underwent a series of treatments to facilitate detailed mineral analysis. Exposure to Natural Conditions: Thin sections were exposed to open air under natural atmospheric conditions. Saturation with Ethylene Glycol: To facilitate the swelling of smectites, thin sections underwent a 12-hour saturation process with ethylene glycol. Heating Process: A heating process at 490°C for 2 hours was employed to characterize heat-sensitive minerals. This specific temperature ensures the destruction of kaolinites while preserving chlorites. The powdered samples and treated thin sections underwent diffractometric analysis using a PANalytical diffractometer, and the resulting data were meticulously processed using specialized Height-score software for thorough interpretation.

3.2.2. X-ray fluorescence (XRF)

We conducted an elemental chemical analysis on the collected samples at the National Office of Mines Tunis. For this purpose, we employed the Perkin-Elmer apparatus, which is equipped with a flame. The apparatus has the flexibility to utilize either acetylene or nitrous oxide-acetylene, adapting to the specific requirements needed for precise and accurate elemental analysis.

4. RESULTS

4.1. Landslides mapping

The AHP analysis revealed the weightage assigned to each parameter, highlighting the slope angle as the most influential factor with a value of 0.309. It was followed by lithofacies at 0.202, and subsequently, distance from roads and terrain elevation, both carrying a weight of 0.119. Conversely, factors such as distance from faults, aspect, land use, and distance from streams displayed lower significance in this analysis. In this study, the calculated consistency ratio stands at 0.015, indicating a satisfactory level of consistency. This level of consistency ensures reliability in determining the weight of each factor, affirming the credibility of the analysis. To construct the Landslide Susceptibility Index (LSI) (Dahoua et al., 2017b), the integration of various causative factors was computed using specific weightings attributed to each factor. The formula utilized for LSI integration involves multiplying each factor by its respective weight: $LSI = \text{Fault density} * 0.073 + \text{Distance to streams} * 0.025 + \text{Slope gradient} * 0.309 + \text{Slope aspect} * 0.075 + \text{Lithofacies} * 0.202 + \text{Plan curvature} * 0.071 + \text{Distance from Roads} * 0.019 + \text{Terrain elevations} * 0.019$ (Table 1). With a consistency ratio of 0.015, the analysis underscores the reliability of the process in determining the weights assigned to each factor, ultimately contributing to the accurate construction of the Landslide Susceptibility Index.

Table 1. Pair-wise comparison matrix and relative weights of causative factor.

Influencing factors	(FD)	(DS)	(SG)	(SA)	(LF)	(PC)	(DR)	(TE)	Weight
Fault density	(FD)	1							0.073
distance to streams	(DS)	1/4	1						0.025
Slope gradient	(SG)	4	7	1					0.309
Slope aspect	(SA)	1	4	1/4	1				0.075
Lithofacies	(LF)	3	6	1/2	3	1			0.202
Plan Curvature	(PC)	1	4	1/4	1	1/3	1		0.071
Distance from roads	(DR)	2	5	1/3	2	1/2	2	1	0.119
Terrain elevations	(TE)	2	5	1/3	2	1/2	2	1	0.119

The landslide susceptibility map produced through the AHP method is depicted in Figure 8a. This map was reclassified into five distinct hierarchical susceptibility classes, as shown in Figure 8b. The susceptibility conditions predominantly range from very high to high along most parts of the deviation road, as illustrated in Figure 8c. This particular area is primarily characterized by steep slopes, which significantly contribute to the heightened susceptibility observed in these regions.

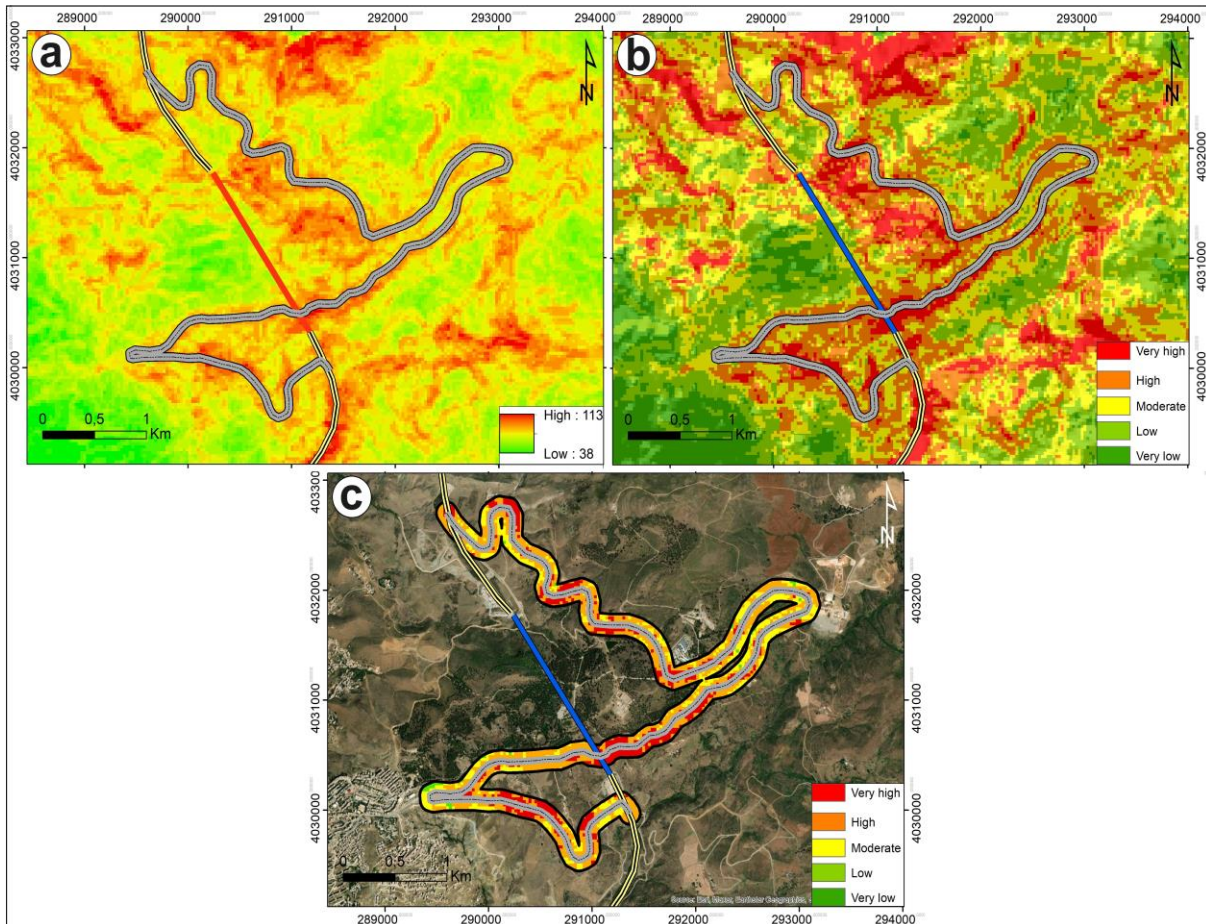


Figure 8. (a) Landslides susceptibility map on the study area in stretched mode; (b) Landslides susceptibility map on the study area in jenks-classified mode; (c) The susceptibility map of the road deviation (for buffer area); (d) Histogram of the susceptibility Classes map of the deviation road (for buffer area).

The area under the curve (AUC) value of 0.93 obtained for the landslide susceptibility map generated through the AHP method signifies a commendable overall success rate, as shown in Figure 9. This metric suggests that the performance of the landslide susceptibility mapping exhibits favorable prediction accuracy across the study area. A value of 0.93 indicates a substantial degree of reliability in predicting and assessing landslide susceptibility, reflecting the effectiveness of the AHP-based methodology in delineating areas prone to landslides within the study area.

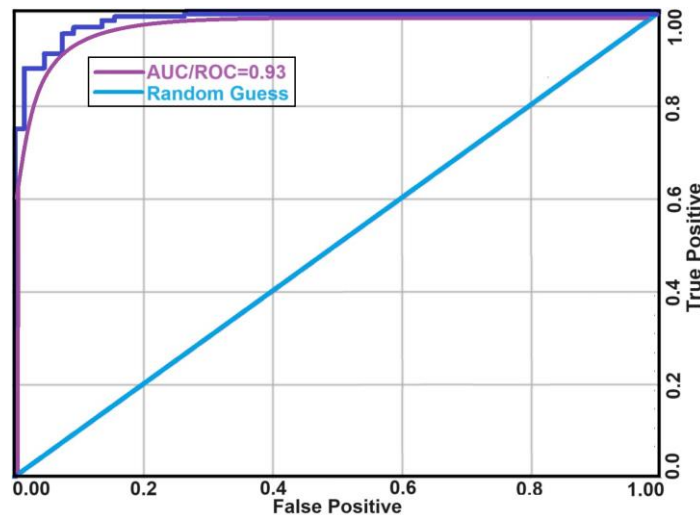


Figure 9. AUC/ROC curve of adopted AHP model.

4.2. Mineral, chemical, and petrographic characters

4.2.1. Mineralogical analyses

The X-ray diffraction (XRD) analysis conducted revealed crucial insights into the mineralogical composition of the samples obtained from the Jebel El Ouahch Tunnel collapse incident. Predominantly, quartz emerged as the primary mineral constituent (Figure 10), demonstrating its prevalent presence within the samples. Moreover, the X-ray fluorescence analysis further validated these findings, highlighting SiO₂ as the principal element, closely followed by Al₂O₃.

The semi-quantitative analysis conducted on all samples unveiled a consistently similar mineralogical distribution pattern. Notably, the samples exhibited a significant proportion of total clays, averaging 43.75% (Table 2). Additionally, quartz emerged as a dominant mineral, accounting for an average of 41.37% across the samples. In addition to quartz, accessory minerals such as feldspar, calcite, dolomite, and traces of iron oxides and siderite were also identified.

Moreover, the diffractograms derived from the oriented samples provided intricate details of the clay mineral assemblage, unveiling the presence of Kaolinite, Illite, Chlorite, Smectite, and regular interstratifications. This extensive mineralogical and geochemical characterization sheds significant light on the composition of the tunnel's geological structure.

The correlation between these identified minerals, particularly the prevalence of quartz and the presence of clay minerals such as Kaolinite and Illite, serves as a pivotal link in understanding the geological vulnerabilities that may have contributed to the collapse incident in the Jebel El Ouahch Tunnel. These findings signify a crucial aspect, indicating that the geological and mineralogical characteristics played a substantial role as one of the primary causes and origins of the tunnel's collapse.

Table 2. Semi-quantitative analysis results.

Minerals	N° Sample		
	S 1-2017	S 2-2017	S 3-2017
Quartz	41	38	44
Argile totale	39	45	40
Feldspath	7	7	5
Calcite	3	2	1
Dolomite	6	4	5
Hématite	1	1	2
Sidérite	2	3	3

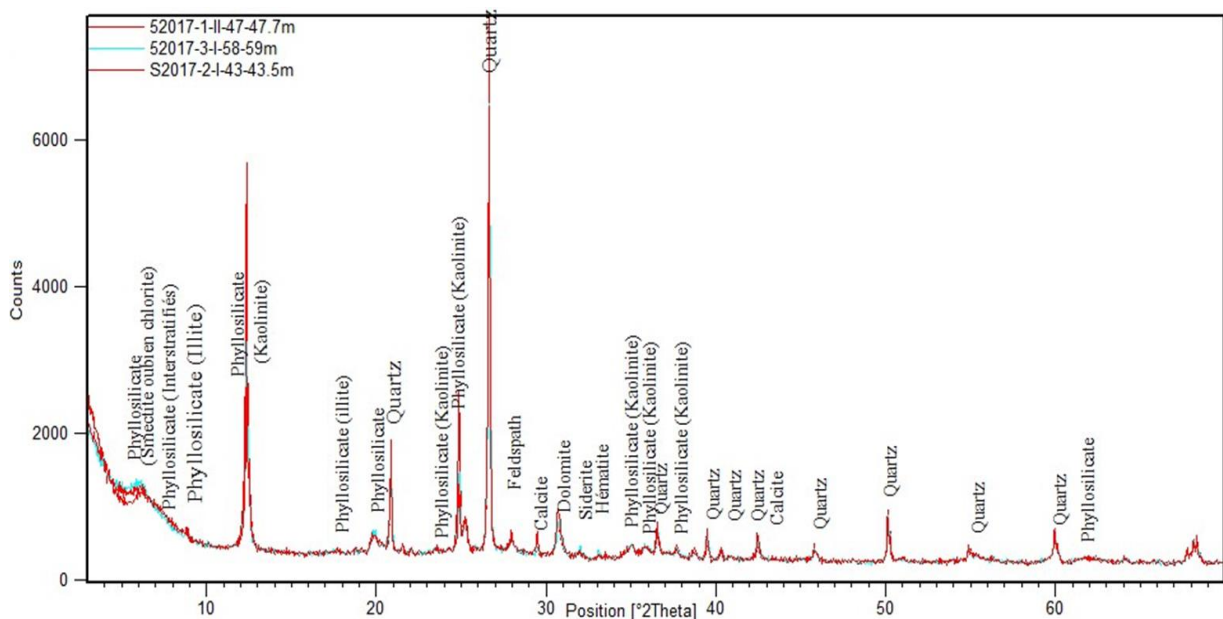


Figure 10. Diffractograms of S1 (drill) samples.

The mineralogical analyses conducted in this study have provided invaluable insights into the composition and distribution of minerals within the collected samples from the Jebel El Ouahch Tunnel collapse incident. Notably, the significant prevalence of quartz and kaolinite, along with the presence of various accessory minerals, provides crucial information regarding the geological characteristics of the analyzed clays. These findings contribute significantly to our understanding of the underlying geological features that could have contributed to the collapse incident. Of particular significance is the identification of multiple clay minerals, which greatly enhances our understanding of their potential influence on the behavior and properties of these clays in various geotechnical and environmental applications.

The semi-quantitative analysis of the clay fraction revealed a dominant presence of kaolinite, constituting approximately 37.92% of the mineral composition. Subsequently, smectite accounted for 20.51%, followed by chlorite at 18.88%, and illite at 13.70%. Additionally, regular interstratifications were observed with an average percentage of 8.99% (Table 3).

Table 3. Percentage of clay minerals.

Minerals	Samples		
	S 1	S 2	S 3
Smectite	34	10	30
Chlorite	18	21	22
Interbedded	4	13	11
Illite	17	19	8
Kaolinite	27	38	28

Understanding the prevalence and distribution of these specific clay minerals, notably the abundance of kaolinite, smectite, chlorite, and illite, provides crucial insights into their potential role as contributing factors to the collapse incident in the Jebel El Ouahch Tunnel. The presence and proportions of these minerals could significantly influence the mechanical behavior and stability of the geological formations, thus underscoring their relevance as key factors in the tunnel's collapse.

4.2.2. Geochemical analysis

The X-ray fluorescence (XRF) analysis, detailed in Table 4, provides crucial insights into the elemental composition of the claystone samples extracted from the Jebel El Ouahch Tunnel collapse incident. Predominantly, the results indicate the substantial presence of Silica (Si) and Aluminum (Al) as the most dominant constituents within the claystone samples. These elements are primarily attributed to the prevalence of quartz (SiO_2) and phyllosilicates, including Kaolinite ($\text{Al}_2\text{Si}_2\text{O}_5(\text{OH})_4$), Illite $[(\text{K}, \text{H}_3\text{O})\text{Al}_2\text{Si}_3\text{AlO}_{10}(\text{OH})_2]$, and chlorite $(\text{Fe}, \text{Mg}, \text{Al})_6(\text{Si}, \text{Al})_4\text{O}_{10}(\text{OH})_8$. Additionally, the analysis indicates the presence of Calcium (Ca) and Magnesium (Mg), primarily associated with calcite and dolomite, albeit in smaller percentages. Notably, the carbonate content exhibited relatively low values of CaCO_3 . Iron (Fe) elements were identified, linked to siderite (FeCO_3) and hematite (Fe_2O_3).

Table 4. Geochemical analyses using XRF.

	S-1 (47.-47.47m)	S-2(43-43,5m)	S-3 (58-59m)
% Al_2O_3	15,3	16,18	14,35
% MgO	2,52	2,48	2,44
% CaO	2,66	2,4	1,94
% Na_2O	0,62	0,59	0,52
% K_2O	1,81	1,3	1,13
% Fe_2O_3	6,55	6,45	6,62
% SiO_2	57,97	57,38	59,84
% PF	9,94	10,77	10,44
% TiO_2	0,88	0,81	0,74

These findings gleaned from the XRF analysis are pivotal in understanding the elemental composition and chemical makeup of the claystone samples. The prevalence of silica, aluminum, and various phyllosilicates, coupled with the presence of accessory minerals such as calcium, magnesium, and iron-bearing minerals, significantly influences the geological and geotechnical behavior of the claystone.

Furthermore, these findings play a pivotal role in assessing the suitability and performance of the claystone in various geological applications. Understanding the chemical composition of these samples provides essential insights into their potential behavior in different environmental conditions. Moreover, these results underscore the importance of geochemical characteristics in evaluating the stability and performance of geological formations, offering valuable insights into the causes and origins underlying the collapse incident in the Jebel El Ouahch Tunnel.

6. DISCUSSION AND INTERPRETATION OF RESULTS

The collapse of the T01 tunnel in Jebel El Ouahch during the excavation phase in January 2014 shed light on the intricate geological and geotechnical challenges of the region. This tunnel traverses folded and fractured greyish claystone formations dating back to the Subnumidian age, which exhibits schistosity and fracture planes distinguished by the presence of kaolinite. Rigorous mineralogical analyses conducted via X-ray diffraction (XRD) unveiled the composition of the claystones, which comprise 43.75% total clay and 41.37% quartz, alongside accessory minerals such as feldspar, calcite, dolomite, and iron oxides (hematite and siderite). Additionally, X-ray fluorescence (XRF) confirmed the prevalence of silica and aluminum, attributed to quartz and phyllosilicates (kaolinite, illite, chlorite, and smectite), while minor percentages of calcium and magnesium were linked to calcite and dolomite, indicating low carbonate content. Fieldwork conducted inside the collapsed tunnel and along its axis revealed the vulnerability of the claystones due to schistosity, micro-folds, and fractures resulting from regional tectonic thrusting. The collapsed section represents a fragile zone, acting as a fault node where the material has disintegrated entirely. Consequently, the characteristics of these claystones deteriorate in this area, leading to the uplifting of the reinforced concrete lining of the tunnel under surrounding rock pressures. Accurate assessment of infrastructure stability, especially for critical public projects like the A1 highway, is of paramount importance in the planning and execution stages. This study employed a comprehensive approach, utilizing GIS-AHP-based modeling alongside geological identification, to generate landslide susceptibility maps along the deviation road impacted by the collapsed T1 tunnel on the A1 highway. Eight influential factors, including lithofacies, slope gradient, slope aspect, elevations, fault density, plan curvature, distance from streams, and distance from roads, were meticulously evaluated, and their specific weights were determined based on their impact. Validation results, analyzed using the ROC (Receiver Operating Characteristic) curve, indicated good acceptability, affirming the model's notable accuracy in predicting landslide susceptibility along the studied road. These landslide susceptibility maps serve as crucial tools for engineers, decision-makers, and planners, aiding in informed decision-making processes to mitigate damage caused by existing or potential landslides. The deviation road, as well as the T01 tunnel of the A1 highway, is in a state of proven instability. It will certainly experience continuous, recurrent, and intense landslides. A radical solution to all the geotechnical issues plaguing this section of the highway is to change the route far away from the Subnumidian formations. Thorough geological and geotechnical studies should precede the initiation of construction for new roads and highways to avert such technical challenges in the future. Tectonic and micro-tectonic aspects warrant thorough consideration in future projects to ensure stability and safety. Implementing proper reinforcement strategies, based on comprehensive studies, will be pivotal in averting similar incidents, ensuring safety, and prolonging the longevity of critical infrastructure projects. While the Analytic Hierarchy Process (AHP) is a widely used multi-criteria decision-making technique for assessing geological hazards, including landslides, it is important to consider its performance and limitations to ensure the reliability and accuracy of the resulting susceptibility maps. AHP facilitates the integration of various factors contributing to landslides, such as slope steepness, environmental conditions, geology, and entropy, enabling the creation of a comprehensive decision support system for assessing landslide susceptibility. The accuracy and reliability of susceptibility mapping using AHP heavily depend on the availability and quality of input data. Incomplete or inaccurate data can result in unreliable susceptibility assessments. The mathematical calculations involved in AHP can be complex, particularly when dealing with multiple criteria and large datasets. This complexity may pose challenges in terms of computational resources and time. The static nature of the model may not account for temporal changes in environmental factors, such as climate change or land-use alterations, which can affect the accuracy of long-term predictions. These susceptibility maps are valuable tools for urban planners and policymakers, providing essential

information for making informed decisions regarding land use zoning and development in landslide-prone areas. They also aid in risk assessment, enabling authorities to take proactive measures for risk mitigation and management, such as implementing preventive measures or issuing warnings. In practical application, our approach includes the assessment of the stability of the A1 deviation road, a temporary sinuous road constructed over a steep relief to address the closure of the East tube and ensure traffic flow. The assessment reveals that the deviation is exposed to 23.87% high risk and 52.04% very high risk. Urgent technical solutions are required to ensure the practicability of the A1 highway in its eastern part, including the consolidation of severe cracks in the 113m section. Tracing a new route should also be considered to address these challenges.

7. CONCLUSIONS AND RECOMMENDATIONS

In conclusion, this manuscript presents a comprehensive study on landslide susceptibility mapping and the geological characterization of a specific area. The research employed the AHP method to assess the relative importance of various factors contributing to landslide susceptibility. The integration of multiple causative factors, including lithofacies, slope angle, distance from roads, and terrain elevation, facilitated the construction of a Landslide Susceptibility Index (LSI). The resulting landslide susceptibility map exhibited favorable prediction accuracy, with a commendable overall success rate indicated by an Area Under the Curve (AUC) value of 0.93.

The significance of this work lies in its practical applications for disaster management and land use planning. By identifying areas prone to landslides, decision-makers can implement preventive measures and adopt appropriate land management strategies. The generated landslide susceptibility map provides valuable information for mitigating the risks associated with slope instability, thus contributing to the safety and sustainable development of the studied area.

One of the advantages of the AHP methodology is its ability to consider multiple factors and assign weights to each factor based on their relative importance. This allows for a comprehensive assessment of landslide susceptibility, considering various influential parameters. Additionally, the integration of GIS technology and statistical analysis tools, such as SPSS, enhances the accuracy and efficiency of the mapping process.

However, it is important to acknowledge the limitations of this study. The selection of factors for landslide susceptibility mapping, although guided by key parameters, lacks rigid guidelines and may vary depending on the specific study area. The accuracy of the susceptibility map is also subject to the quality of input data and the assumptions made during the analysis. Therefore, careful consideration should be given to data collection, preprocessing, and validation to ensure reliable results.

Future work in this field could focus on refining the methodology by incorporating additional factors, refining the weightings assigned to existing factors, or applying other probabilistic methods. Advancements in GIS techniques and data availability can further enhance the accuracy and efficiency of landslide susceptibility mapping. Long-term monitoring and validation efforts are crucial to continuously improve the reliability of the models and ensure their effectiveness in real-world applications. Additionally, investigating the temporal dynamics of landslide susceptibility and considering the impact of climate change could provide valuable insights for proactive landslide risk management in a changing environment.

ACKNOWLEDGMENT

This work was conducted under the supervision of the Laboratory of Applied Research in Engineering Geology, Geotechnics, Water Sciences, and Environment at Setif 1 University, Algeria. We would like to express our gratitude to the DGRSDT-MESRS for their support.

USE OF AI TOOLS DECLARATION

The authors declare they have not used Artificial Intelligence (AI) tools in the creation of this article.

AUTHOR CONTRIBUTIONS

All authors contributed equally to this work. All authors read and approved the final manuscript.

CONFLICTS OF INTEREST

The authors declare no conflict of interest.

REFERENCE

- Achour, Y., Boumezbeur, A., Hadji, R., Chouabbi, A., Cavaleiro, V., & Bendaoud, E. A. (2017). Landslide susceptibility mapping using analytic hierarchy process and information value methods along a highway road section in Constantine, Algeria. *Arabian Journal of Geosciences*, *10*, 1–16. <https://doi.org/10.1007/s12517-017-2980-6>
- Achour, Y., & Pourghasemi, H. R. (2020). How do machine learning techniques help in increasing accuracy of landslide susceptibility maps? *Geoscience Frontiers*, *11*(3), 871–883. <https://doi.org/10.1016/j.gsf.2019.10.001>
- Achour, Y., Saidani, Z., Touati, R., Pham, Q. B., Pal, S. C., Mustafa, F., & Balik Sanli, F. (2021). Assessing landslide susceptibility using a machine learning-based approach to achieving land degradation neutrality. *Environmental Earth Sciences*, *80*, 1–20. <https://doi.org/10.1007/s12665-021-09889-9>
- Aicha, B., Mezhoud, S., Karech, T., & B eroual, A. (2022). Numerical Analysis of the Dynamic Behavior of Shallow Tunnel: a Case Study of Djebel El-Ouahch Tunnel, Algeria. *Transportation Infrastructure Geotechnology*, *9*(3), 385–401. <https://doi.org/10.1007/s40515-021-00183-6>
- Anis, Z., Wissem, G., Riheb, H., Biswajeet, P., & Essghaier, G. M. (2019). Effects of clay properties in the landslides genesis in flysch massif: Case study of A in Draham, North Western Tunisia. *Journal of African Earth Sciences*, *151*, 146–152. <https://doi.org/10.1016/j.jafrearsci.2018.12.005>
- Ayalew, L., Yamagishi, H., Marui, H., & Kanno, T. (2005). Landslides in Sado Island of Japan: Part II. GIS-based susceptibility mapping with comparisons of results from two methods and verifications. *Engineering geology*, *81*(4), 432–445. <https://doi.org/10.1016/j.enggeo.2005.08.004>
- Bagwan, W. A., Gavali, R. S., & Maity, A. (2023). Quantifying soil organic carbon (SOC) density and stock in the Urmodi River watershed of Maharashtra, India: implications for sustainable land management. *Journal of Umm Al-Qura University for Applied Sciences*, 1–17. <https://doi.org/10.1007/s43994-023-00064-3>.
- Benmarce, K., Hadji, R., Zahri, F., Khanchoul, K., Chouabi, A., Zighmi, K., & Hamed, Y. (2021). Hydrochemical and geothermometry characterization for a geothermal system in semiarid dry climate: The case study of Hamma spring (Northeast Algeria). *Journal of African Earth Sciences*, *182*, 104285. <https://doi.org/10.1016/j.jafrearsci.2021.104285>
- Benyoucef, A. A., Gadri, L., Hadji, R., Slimane, H., Mebrouk, F., & Hamed, Y. (2023). Empirical graphical and numerical model for the schematization of underground mining operations in the heterogeneous rock masses, case of Boukhadra mine, NE Algeria. *Arabian Journal of Geosciences*, *16*(3), 165. <https://doi.org/10.1007/s12517-023-11219-1>
- Bonini, M., & Barla, G. (2012). The Saint Martin La Porte access adit (Lyon–Turin Base Tunnel) Tunnelling and underground space technology, *30*, 38–54. <https://doi.org/10.1016/j.tust.2012.02.004>
- Boubazine, L., Boumazbeur, A., Hadji, R., & Fares, K. (2022). Slope failure characterization: A joint multi-geophysical and geotechnical analysis, case study of Babor Mountains range, NE Algeria. *Mining of Mineral Deposits*, *16*(4). <https://doi.org/10.33271/mining16.04.065>.
- Boulema, S., Hadji, R., & Hamimed, M. (2021). Depositional environment of phosphorites in a semiarid climate region, case of El Kouif area (Algerian–Tunisian border). *Carbonates and Evaporites*, *36*(3), 53. <https://doi.org/10.1007/s13146-021-00719-4>
- Chen, L. L., Wang, Z. F., & Wang, Y. Q. (2022). Failure analysis and treatments of tunnel entrance collapse due to sustained rainfall: a case study. *Water*, *14*(16), 2486. <https://doi.org/10.3390/w14162486>
- Conforti, M., & Ietto, F. (2021). Modeling shallow landslide susceptibility and assessment of the relative importance of predisposing factors, through a GIS-based statistical analysis. *Geosciences*, *11*(8), 333. <https://doi.org/10.3390/geosciences11080333>
- Cullity, B. D. (1956). *Elements of X-ray Diffraction*. Addison-Wesley Publishing Company.
- Dahoua, L., Savenko V.Y., Hadji, R. (2017a). GIS-based technic for roadside-slope stability assessment: an bivariate approach for A1 East-west highway, North Algeria. *Mining Science* *24*, 117–127. <https://doi.org/10.5277/msc172407>
- Dahoua, L., Yakovitch, S.V., Hadji, R., & Farid, Z. (2017b) Landslide Susceptibility Mapping Using Analytic Hierarchy Process Method in BBA-Bouira Region, Case Study of East-West Highway, NE Algeria. In A.

- Kallel, M., Ksibi, H., Ben Dhia & N. Khélifi (Eds.), *Recent Advances in Environmental Science from the Euro-Mediterranean and Surrounding Regions* (pp.1837-1840). Proceedings of Euro-Mediterranean Conference for Environmental Integration (EMCEI-1), Tunisia 2017. Springer, Cham. <https://doi.org/10.1007/978-3-319-70548-4>
- Dahoua, L., Usychenko, O., Savenko, V. Y., & Hadji, R. (2018). Mathematical approach for estimating the stability of geotextile-reinforced embankments during an earthquake. *Mining Science*, *25*, 207–217. <https://doi.org/10.5277/msc182501>
- El Mekki, A., Hadji, R., & Chemseddine, F. (2017). Use of slope failures inventory and climatic data for landslide susceptibility, vulnerability, and risk mapping in souk Ahras region. *Mining Science*, *24*, 117–127. <https://doi.org/10.5277/msc172417>
- Feng, X., & Jimenez, R. (2015). Predicting tunnel squeezing with incomplete data using Bayesian networks. *Engineering Geology*, *195*, 214–224. <https://doi.org/10.1016/j.enggeo.2015.06.017>
- Fredj, M., Hafsaoui, A., Riheb, H., Boukarm, R., & Saadoun, A. (2020). Back-analysis study on slope instability in an open pit mine (Algeria). *Naukovyi Visnyk Natsionalnoho Hirnychoho Universytetu*, (2), 24–29. <https://doi.org/10.33271/nvngu/2020-2/024>
- Guzzetti, F. (2021). On the Prediction of Landslides and Their Consequences. In K. Sassa, M. Mikos, S. Sassa, P.T. Bobrowsky, K. Takara, K. Dang (Eds) *Understanding and Reducing Landslide Disaster Risk* (3–32). Volume 1, Sendai Landslide Partnerships and Kyoto Landslide Commitment. Springer International Publishing, Cham. https://doi.org/10.1007/978-3-030-60196-6_1
- Hadji, R., Limani, Y., Baghem, M., & Demdoum, A. (2013). Geologic, topographic and climatic controls in landslide hazard assessment using GIS modeling: a case study of Souk Ahras region, NE Algeria. *Quaternary International*, *302*, 224–237. <https://doi.org/10.1016/j.quaint.2012.11.027>
- Hadji, R., Limani, Y., & Demdoum, A. (2014, b). Using multivariate approach and GIS applications to predict slope instability hazard case study of Machrouha municipality, NE Algeria. In *2014 1st International Conference on Information and Communication Technologies for Disaster Management (ICT-DM)* (pp. 1–10). IEEE. DOI: 10.1109/ICT-DM.2014.6917787
- Hadji, R., Limani, Y., Boumazbeur, A. E., Demdoum, A., Zighmi, K., Zahri, F., & Chouabi, A. (2014). Climate change and its influence on shrinkage–swelling clays susceptibility in a semi-arid zone: a case study of Souk Ahras municipality, NE-Algeria. *Desalination and Water Treatment*, *52* (10–12), 2057–2072. <https://doi.org/10.1080/19443994.2013.812989>
- Hadji, R., Chouabi, A., Gadri, L., Raïs, K., Hamed, Y., & Boumazbeur, A. (2016). Application of linear indexing model and GIS techniques for the slope movement susceptibility modeling in Bousselam upstream basin, Northeast Algeria. *Arabian Journal of Geosciences*, *9*, 1–18. <https://doi.org/10.1007/s12517-015-2169-9>
- Hadji, R., Raïs, K., Gadri, L., Chouabi, A., & Hamed, Y. (2017). Slope failure characteristics and slope movement susceptibility assessment using GIS in a medium scale: a case study from Ouled Driss and Machrouha municipalities, Northeast Algeria. *Arabian Journal for Science and Engineering*, *42*, 281–300. <https://doi.org/10.1007/s13369-016-2046-1>
- Hamed, Y., Hadji, R., Ahmadi, R., Ayadi, Y., Shuhab, K., & Pulido-Bosch, A. (2023). Hydrogeological investigation of karst aquifers using an integrated geomorphological, geochemical, GIS, and remote sensing techniques (Southern Mediterranean Basin—Tunisia). *Environment, Development and Sustainability*, 1–33. <https://doi.org/10.1007/s10668-023-02994-8>
- Hoek, E. (2001). Big tunnels in bad rock. *Journal of Geotechnical and Geoenvironmental Engineering*, *127*(9), 726–740. [https://doi.org/10.1061/\(ASCE\)1090-0241\(2001\)127:9\(726\)](https://doi.org/10.1061/(ASCE)1090-0241(2001)127:9(726))
- Kallel, A., Ksibi, M., Dhia, H. B., & Khélifi Nabil (Eds.) (2018). *Recent advances in environmental science from the euro-mediterranean and surrounding regions: Proceedings of Euro-Mediterranean Conference for Environmental Integration (EMCEI-1) Tunisia 2017*. Volume I and Volume II. Springer. <https://doi.org/10.1007/978-3-319-70548-4>
- Karim, Z., Hadji, R., & Hamed, Y. (2019). GIS-based approaches for the landslide susceptibility prediction in Setif Region (NE Algeria). *Geotechnical and Geological Engineering*, *37*(1), 359–374. <https://doi.org/10.1007/s10706-018-0615-7>
- Kerbati, N. R., Gadri, L., Hadji, R., Hamad, A., & Boukelloul, M. L. (2020). Graphical and numerical methods for stability analysis in surrounding rock of underground excavations, example of Boukhadra Iron Mine NE Algeria. *Geotechnical and Geological Engineering*, *38*, 2725–2733. <https://doi.org/10.1007/s10706-019-01181-9>
- Kimour, M., Boukelloul, M. L., Hafsaoui, A., Narsis, S., Benghadab, K. M., & Benselhou, A. (2023). Geomechanical characterization of rock mass rating and numerical modeling for underground mining excavation design. *Journal of Geology, Geography and Geoecology*, *32*(1), 67–78.

- <https://doi.org/10.15421/112308>
- Kitchah, F., Benmebarek, S., & Djabri, M. (2021). Numerical assessment of tunnel collapse: a case study of a tunnel at the East–West Algerian highway. *Bulletin of Engineering Geology and the Environment*, 80, 6161–6176. <https://doi.org/10.1007/s10064-021-02318-y>
- Leichnetz, W. (1990). Analysis of collapses on tunnel construction sites on the new lines of the German Federal Railway. *Tunnelling and underground space technology*, 5(3), 199–203. [https://doi.org/10.1016/0886-7798\(90\)90007-7](https://doi.org/10.1016/0886-7798(90)90007-7)
- Lin, D., Yuan, R., Shang, Y., Bao, W., Wang, K., Zhang, Z., Li, K., & He, W. (2017). Deformation and failure of a tunnel in the restraining bend of a strike–slip fault zone: an example from Hengshan Mountain, Shanxi Province, China. *Bulletin of Engineering Geology and the Environment*, 76, 263–274. <https://doi.org/10.1007/s10064-016-0850-1>
- Mahdadi, F., Boumezbeur, A., Hadji, R., Kanungo, D. P., & Zahri, F. (2018). GIS-based landslide susceptibility assessment using statistical models: a case study from Souk Ahras province, NE Algeria. *Arabian Journal of Geosciences*, 11, 476, 1–21. <https://doi.org/10.1007/s12517-018-3770-5>
- Manchar, N., Benabbas, C., Hadji, R., Bouaicha, F., & Grecu, F. (2018). Landslide susceptibility assessment in Constantine region (NE Algeria) by means of statistical models. *Studia Geotechnica et Mechanica*, 40(3), 208–219. <https://doi.org/10.2478/sgem-2018-0024>
- Manchar, N., Hadji, R., Bougherara, A., & Boufaa, K. (2022). Assessment of relative-active tectonics in rhumel-smendou basin (ne Algeria)–observations from the morphometric indices and hydrographic features obtained by the digital elevation model. *Geomatics, Landmanagement and Landscape*, 4, 47–65. <http://dx.doi.org/10.15576/GLL/2022.4.47>
- Moretti, E., Coccioni, R., Guerrero, F., Lahondère, J. C., Loiacono, F., & Puglisi, D. (1991). The numidian sequence between guelma and constantine (eastern tell, Algeria). *Terra Nova*, 3(2), 153–165. <https://doi.org/10.1111/j.1365-3121.1991.tb00868.x>
- Ncibi, K., Hadji, R., Hajji, S., Besser, H., Hajlaoui, H., Hamad, A., Mokadem, N., Saad, A.B., Hamdi, M., & Hamed, Y. (2021). Spatial variation of groundwater vulnerability to nitrate pollution under excessive fertilization using index overlay method in central Tunisia (Sidi Bouzid basin). *Irrigation and Drainage*, 70(5), 1209–1226. <https://doi.org/10.1002/ird.2599>
- Qiao, S., Cai, Z., Tan, J., Xu, P., & Zhang, Y. (2020). Analysis of collapse mechanism and treatment evaluation of a deeply buried hard rock tunnel. *Applied Sciences*, 10(12), 4294. <https://doi.org/10.3390/app10124294>
- Reichenbach, P., Rossi, M., Malamud, B. D., Mihir, M., & Guzzetti, F. (2018). A review of statistically-based landslide susceptibility models. *Earth-Science Reviews*, 180, 60–91. <https://doi.org/10.1016/j.earscirev.2018.03.001>
- Saadoun, A., Yilmaz, I., Hafsaoui, A., Hadji, R., Fredj, M., Boukarm, R., & Nakache, R. (2020). Slope stability study in quarries by different approaches: case Chouf Amar Quarry, Algeria. *IOP Conference Series: Materials Science and Engineering*, 960, 042026. DOI:10.1088/1757-899X/960/4/042026
- Saaty, T. L. (1977). A scaling method for priorities in hierarchical structures. *Journal of mathematical psychology*, 15(3), 234–281. [https://doi.org/10.1016/0022-2496\(77\)90033-5](https://doi.org/10.1016/0022-2496(77)90033-5)
- Saaty, T. (1980). *The analytic hierarchy process (AHP) for decision making*. Kobe, Japan (1–69).
- Taib, H., Benabbas, C., Khiari, A., Hadji, R., & Haythem, D. (2022). Geomatics-based assessment of the neotectonic landscape evolution along the Tebessa-Morsott-Youkous collapsed basin, Algeria. *Geomatics, Landmanagement and Landscape*, (3), 131–146. <http://dx.doi.org/10.15576/GLL/2022.3.131>
- Taib, H., Hadji, R., Hamed, Y., Bensalem, M. S., & Bensalem, A. S. (2023a). Exploring neotectonic activity in a semiarid basin: a case study of the Ain Zerga watershed. *Journal of Umm Al-Qura University for Applied Sciences*. <https://doi.org/10.1007/s43994-023-00072-3>
- Taib, H., Hadji, R., & Hamed, Y. (2023b). Erosion patterns, drainage dynamics, and their environmental implications: a case study of the hammamet basin using advanced geospatial and morphometric analysis. *Journal of Umm Al-Qura University for Applied Sciences*, 1–16. <https://doi.org/10.1007/s43994-023-00096-9>
- Zahri, F., Boukelloul, M. L., Hadji, R., & Talhi, K. (2016). Slope stability analysis in open pit mines of Jebel Gustar career, NE Algeria—a multi-steps approach. *Mining Science*, 23, 137–146. DOI:10.5277/msc162311
- Zeqiri, R. R., Riheb, H., Karim, Z., Younes, G., Rania, B., & Aniss, M. (2019). Analysis of safety factor of security plates in the mine "Trepça" Stantërg. *Mining Science*, 26, 21–36. DOI:10.37190/msc192602
- Zerzour, O., Gadri, L., Hadji, R., Mebrouk, F., & Hamed, Y. (2020). Semi-variograms and kriging techniques in iron ore reserve categorization: application at Jebel Wenza deposit. *Arabian Journal of Geosciences*, 13, 820. <https://doi.org/10.1007/s12517-020-05858-x>

- Zerzour, O., Gadri, L., Hadji, R., Mebrouk, F., & Hamed, Y. (2021). Geostatistics-Based Method for Irregular Mineral Resource Estimation, in Ouenza Iron Mine, Northeastern Algeria. *Geotechnical and Geological Engineering*, 39(5), 3337–3346. <https://doi.org/10.1007/s10706-021-01695-1>
- Zêzere, J. L., Pereira, S., Melo, R., Oliveira, S. C., & Garcia, R. A. (2017). Mapping landslide susceptibility using data-driven methods. *Science of the total environment*, 589, 250–267. <https://doi.org/10.1016/j.scitotenv.2017.02.188>
- Zhang, G. H., Jiao, Y. Y., Chen, L. B., Wang, H., & Li, S. C. (2015). Analytical model for assessing collapse risk during mountain tunnel construction. *Canadian Geotechnical Journal*, 53(2), 326–342. <https://doi.org/10.1139/cgj-2015-0064>



© 2023 by the author(s). This article is an open access article distributed under the terms and conditions of the Creative Commons Attribution-NonCommercial (CC-BY-NC) license (<http://creativecommons.org/licenses/by/4.0/>).